Hindawi
Mathematical Problems in Engineering
Volume 2022, Article ID 5472105, 15 pages
https://doi.org/10.1155/2022/5472105

Research Article

Trajectory Optimization of Multi-UAVs for Marine Target Tracking during Approaching Stage

Hao-Ran Shi, Fa-Xing Lu, Ling Wu, and Jia-Wei Xia

Naval University of Engineering, Wuhan 430033, China

Correspondence should be addressed to Hao-Ran Shi; naroahux@163.com

Received 24 April 2022; Revised 29 October 2022; Accepted 15 November 2022; Published 26 December 2022

Academic Editor: Zhenbo Wang

This paper focuses on a coordinated tracking planning method of multiple unmanned aerial vehicles (UAVs), which was deployed in the best positions to better fulfill the marine target localization tasks when approaching the target. The optimal planning of multi-UAVs was implemented using an online centralized nonlinear model predictive control (NMPC) based on the target state's uncertainty criteria. The penalty function is used to solve UAV platform dynamic performance in the model predictive control method to consider the more realistic situation. The coordinated planning problems of multi-UAVs are numerically simulated and compared with the Lyapunov vector field guidance (LVFG) method under classical mission scenarios. Simulation results demonstrate that the algorithm can maintain the optimal observation configuration of multi-UAVs to improve the marine target positioning accuracy, verifying the feasibility and superiority of this method. Furthermore, the simulation results can provide a useful reference for the flight control law design of multi-UAVs with optimal observation configuration.

1. Introduction

Recently, organized conflict occurred frequently in the maritime arena, threatening the safe passing of ships from the exclusive economic zones (EEZ). Therefore, powerful security surveillance is expected for the remote marine target in the EEZ [1]. UAVs are widely used in intelligence surveillance, early warning, communication, attack, and other aspects because of their various sensors, concealed actions, controllable cost, and needlessness for personnel, which has the potential to provide an accurate indication of the remote marine target [2, 3]. The sensor must obtain more target information to gain a precise state of the remote maritime target. As a result, this paper will study the location and tracking of the remote marine target by multi-UAVs based on angle and range measurements.

Many works have been carried out on target location and tracking based on UAVs. To effectively use the observation information, Pack et al. [4] used the Kalman filter algorithm to estimate its state. Wang et al. [5] realized target fusion estimation using a distributed unscented information filter. The detection data was combined using an adaptive IMM-information filtering technique by Zhang et al. [6]. Another important field of multi-UAVs' coordinated positioning is to enhance the target state estimation by studying multi-UAVs' position configuration. The Fisher information matrix (FIM) and its inverse matrix, Cramer–Rao lower bound, (CRLB) are the popularly used criteria for evaluating target position accuracy. The optimal observation configuration can be classified into two types, namely, A-optimal and D-optimal. A-optimal seeks to minimize the trace of the FIM's inverse, whereas D-optimal seeks to maximize the FIM's determinant. Bishop et al. [7] investigated the best sensor-target geometries for range-only, time-of-arrival, and bearing-only localization using D-optimal. Zhong et al. [8] analyzed the optimal configuration of sensor-target geometries in three-dimensional space using D-optimal. Xu and Dogancay [9] explored the sensor placement problem for AOA observation in three-dimensional space utilizing A-optimal. However, the criteria based on FIM must calculate the expression of FIM, and the calculation becomes more complex as the dimension and number of UAVs increase. As a result, the information entropy is used in this paper. According to Grocholsky et al. [10], Hoffmann and Tomlin [11], and

Darmon [12], entropy was defined to measure the amount of uncertainty in-state results and was used as the cost function to control the observation configuration of UAVs.

Another problem of coordinated location and tracking based on multi-UAVs is controlling UAVs and maintaining the observation configuration to obtain the optimal target estimation. Many research studies have been carried out to solve the trajectory optimization problem of UAVs [13, 14]. Frew et al. [15] used the LVFG method to control multi-UAVs to keep standoff tracking of stationary and moving targets. Lim et al. [16] presented a strategy for standoff target tracking by a team of unmanned aircraft using vector field, which is only to maintain the optimal observation during the hovering phase. Using the vector field approach, Jung et al. [17] proposed path following, arrival position, angle, and time control. Sinclair et al. [18] proposed a suboptimal feedback guidance law that keeps the sight angle of the sensor and the target 90 degrees while ensuring that the sensor is close to the target. These are all based on the coordinated tracking of two UAVs. Zhao et al. [19] discussed the cooperative control of multi-UAVs in the case of only angle measurement. Hu et al. [20] and Wang et al. [21] realized the coordinated optimal target tracking of multi-UAVs using the receding horizon control method, which did not consider the observation of multi-UAVs based on angle and range measurements.

Until now, most of the existing studies only focused on finding the necessary conditions for UAVs' placement optimality, but very few have considered the concrete solution process of coordinated control multi-UAVs based on angle and range measurements. Moreover, most existing works only consider the optimal placement when UAVs circle around the target; very few studies in the literature have evaluated the optimal placement of multiple UAVs approaching the target. However, it is difficult for UAVs to make hovering motions for the remote marine target in practical applications. UAVs are expected to keep optimal observation while approaching the target. Naturally, two closely related problems can arise in the optimal UAV placement for remote marine target localization. The first is to determine the cost function of the observation based on angle and range measurements when the UAV approaches the target. The second is solving the optimal control command so that UAVs can be deployed in the best positions to better fulfill the target localization tasks.

Motivated by the aforementioned aspects, this paper focuses on multi-UAVs' coordinated optimal observation problems based on angle and range measurements for the remote marine target. Firstly, the cost function based on information theory is derived, and then the NMPC method is used to solve the optimal control problem of multi-UAVs with constraint variables. Finally, the simulation results of the coordinated tracking of multi-UAVs in four cases are displayed. The results show that the algorithm proposed in this paper can increase the measurement information and reduce the uncertainty of target state estimation to achieve accurate target localization.

2. Problem Definition

2.1. UAV Dynamic Model. Currently, the mathematical model of UAVs with autopilot is generally used in the coordinated control of UAVs, which has the advantage of engineering practicability. It is assumed that each UAV has a low-level flight controller, which controls the UAV's yaw rate and velocity through control commands to control the UAV's flight status. We consider a two-dimensional UAV kinematic model as [22]

$$\begin{pmatrix} \dot{x} \\ \dot{y} \\ \dot{\psi} \\ \dot{v} \\ \dot{\omega} \end{pmatrix} = f(\mathbf{x}, \mathbf{u}) = \begin{pmatrix} v\cos\psi \\ v\sin\psi \\ \omega \\ -\dfrac{1}{\tau_v}v + \dfrac{1}{\tau_v}u_v \\ -\dfrac{1}{\tau_\omega}v + \dfrac{1}{\tau_\omega}u_\omega \end{pmatrix}, \tag{1}$$

where $\mathbf{x} = [x, y, \psi, v, \omega]^T$ represent the inertial position, heading, speed, and yaw rate of the UAV, respectively. τ_v and τ_ω are time-delay constants related to the UAV and its flight status. $\mathbf{u} = [u_v, u_\omega]^T$ is the control input of the UAV, which represents the control command of the speed and the yaw rate, respectively, with the following dynamic limits of the UAV:

$$\begin{aligned} |u_v - v_0| &\le \Delta v_{\max}, \\ |u_\omega| &\le \omega_{\max}, \end{aligned} \tag{2}$$

where v_0 is a cruise speed of the UAV and $\Delta v_{\max}$ and $\omega_{\max}$ represent the maximum change range of UAV cruise speed and turning rate, respectively. To design the nonlinear model predictive controller, the continuous UAV model in (1) can be discretized by Euler integration into

$$\mathbf{x}_{k+1} = f_d(\mathbf{x}_k, \mathbf{u}_k) = \mathbf{x}_k + T_s f(\mathbf{x}_k, \mathbf{u}_k), \tag{3}$$

where $\mathbf{x}_k = [x_k, y_k, \psi_k, v_k, \omega_k]^T$, $\mathbf{u}_k = [u_{vk}, u_{\omega k}]^T$, and T_s is a sampling time.

2.2. Target Model. The remote marine target is mainly aimed at the relatively slow-moving target such as the warship. Taking the uniform linear motion model as an example, the target's motion model in the two-dimensional plane is established. $\mathbf{x}(k) = [x(k), \dot{x}(k), y(k), \dot{y}(k)]^T$ represent that the state of the target includes position and speed, and then the system state can be expressed in the following form [23]:

$$\mathbf{x}(k) = F(k)\mathbf{x}(k-1) + G(k)w(k), \tag{4}$$

where

$$F(k-1)=\begin{bmatrix}1 & T_s & 0 & 0\\ 0 & 1 & 0 & 0\\ 0 & 0 & 1 & T_s\\ 0 & 0 & 0 & 1\end{bmatrix},$$
$$G(k-1)=\begin{bmatrix}0.5{T_s}^2 & 0\\ T_s & 0\\ 0 & 0.5{T_s}^2\\ 0 & T_s\end{bmatrix}, \tag{5}$$

$w(k)$ is gaussian process noise with zero mean and the covariance matrix of process noise is Q_k.

2.3. Sensor Model. The measurement z of the sensor can be modeled according to the position of the UAV $(x, y)^T$ and the target position $(x_t, y_t)^T$ as follows:

$$z(k)=h\left(\mathbf{x}_k,\mathbf{x}_{t,k}\right)+v_k=\begin{pmatrix}\sqrt{\left(x_{t,k}-x_k\right)^2+\left(y_{t,k}-y_k\right)^2}\\ \tan^{-1}\dfrac{y_{t,k}-y_k}{x_{t,k}-x_k}\end{pmatrix}+v_k, \tag{6}$$

where v_k is gaussian measurement noise with zero mean, and the measurement noise covariance matrix is R_k, $R_k=\begin{bmatrix}\sigma_r^2 & 0\\ 0 & \sigma_\phi^2\end{bmatrix}$.

2.4. Extended Information Filtering (EIF). Compared with the extended Kalman filter (EKF) [24], EIF can easily realize the information matrix fusion. The simple addition of nature makes information filtering very suitable for multisensor, decentralized, and distributed estimation. Each sensor node only needs to generate an information matrix, and the global information estimation can be obtained by simple algebraic addition at the fusion center. The state estimate $\hat{x}$ and covariance P are used in EKF, which are replaced by the information state $\hat{y}$ and information matrix Y in the information form. The information state and information matrix are defined as $\hat{y}=P^{-1}\hat{x}$, $Y=P^{-1}$. EIF includes prediction process and the estimation process as follows [20]:

Prediction process:

$$Y(k|k-1)=\left[F(k)Y^{-1}(k-1|k-1)F^T(k)+Q(k)\right]^{-1}, \tag{7}$$

$$\hat{y}(k|k-1)=Y(k|k-1)F(k)\hat{x}(k-1|k-1). \tag{8}$$

Definition:

$$I_i(k)=H_i^T(k)R_i^{-1}(k)H_i(k), \tag{9}$$

$$i_i(k)=H_i^T(k)R_i^{-1}(k)\left[z_i(k)-h_i\left(x_k,x_{t,k}\right)+H_i(k)\hat{x}(k|k-1)\right], \tag{10}$$

$$\hat{x}(k|k-1)=Y^{-1}(k|k-1)\hat{y}(k|k-1). \tag{11}$$

Estimation process:

$$Y(k|k)=Y(k|k-1)+\sum_{i=1}^{n}I_i(k), \tag{12}$$

$$\hat{y}(k|k)=\hat{y}(k|k-1)+\sum_{i=1}^{n}i_i(k), \tag{13}$$

$$\hat{x}(k|k)=Y^{-1}(k|k)\hat{y}(k|k), \tag{14}$$

$\hat{y}(k|k-1)$ and $Y(k|k-1)$ are prediction information state and prediction information matrix, respectively, $Y(k-1|k-1)$ is the information state matrix of $k-1$ moment, $H_i(k)$ is the Jacobian matrix of the UAV i, and $z_i(k)$ is measurement information of UAV i.

3. Nonlinear Model Predictive Control

3.1. Choice of Cost Function. Shannon defined entropy in information theory to measure the amount of uncertainty or randomness in-state results. Entropy is the most general measure of uncertainty in sensing and estimation tasks. The larger the entropy, the less accurate the state estimation. Conversely, the smaller the entropy, the more accurate the target state estimation will be. An additional benefit is choosing information entropy as a cost function in controlling multiple sensors. The entropy of the estimated distribution with multiple sensor observations can be decomposed according to the observed mutual information, which provides a beneficial structure for multiple sensor cooperation, as shown in EIF. Next, we will analyze the relationship between the information entropy and the covariance matrix.

The probability density function of target state X is $p(x|z_1,z_2,z_i)$; after EIF and obeying normal distribution $N(\mu,P)$, we can get the probability density function of n-dimensional random variable X as

$$p(x|z_1,z_2,z_i)=\frac{1}{\sqrt{(2\pi)^n\det(P)}}\exp\left(-\frac{1}{2}(x-\mu)^TP^{-1}(x-\mu)\right), \tag{15}$$

where μ and P are Gaussian of mean and covariance after EIF, respectively. We define $H(p(x|z_1,z_2,z_i))$ to be the entropy of the estimate distribution, according to the definition of entropy:

$$\begin{aligned} H(p(x|z_1,z_2,z_i)) &= -\int_{-\infty}^{\infty} p(x|z_1,z_2\ldots,z_i)\log p(x|z_1,z_2,z_i)d(x|z_1,z_2\ldots,z_i) \\ &= -\int_{-\infty}^{\infty} p(x|z_1,z_2\ldots,z_i)\log\left[(2\pi)^{-n/2}|P|^{-1/2}\exp\left(-\frac{1}{2}(x-\mu)^T P^{-1}(x-\mu)\right)\right]d(x|z_1,\ldots z_2,z_i) \\ &= -\int_{-\infty}^{\infty} p(x|z_1,z_2\ldots,z_i)\left[\log\left((2\pi)^{-n/2}|P|^{-1/2}\right)-\frac{1}{2}(x-\mu)^T P^{-1}(x)-(\mu)\log e\right]d(x|z_1,z_2\ldots,z_i) \\ &= \log\left((2\pi)^{-n/2}|P|^{-1/2}\right)+\frac{\log e}{2}\int_{-\infty}^{\infty}(x-\mu)^T P^{-1}(x-\mu)d(x|z_1,z_2\ldots,z_i). \end{aligned} \tag{16}$$

Let $x = P^{1/2}y + \mu$, we can get $y \sim N(0,1)$ and

$$\begin{aligned} H(p)(x|z_1,z_2\ldots,z_i) &= \log\left((2\pi)^{-(n/2)}|P|^{-(1/2)}\right)+\frac{\log e}{2}\int_{-\infty}^{\infty}p(y)\times y^T y dy \\ &= \log\left((2\pi)^{-n/2}|P|^{-(1/2)}\right)+\frac{\log e}{2}\sum_{i=1}^{n}E\left[y_i^2\right] \\ &= \log\left((2\pi)^{n/2}|P|^{(1/2)}\right)+\frac{n\log e}{2} \\ &= \frac{1}{2}\log\left[(2\pi e)^n|P|\right]. \end{aligned} \tag{17}$$

Equation (17) shows that the target state's entropy is proportional to the determinant of the covariance matrix. To obtain an accurate target state, the determinant of the covariance matrix needs to be as small as possible, corresponding to the determinant of the information matrix being as large as possible, and the performance function could be as follows:

$$J_{i,k} = -\left|Y_{i,k}\right|. \tag{18}$$

Therefore, the entropy minimization control problem is transformed into the control problem of minimizing the negative value of the information matrix's determinant.

3.2. Model Predictive Control Method. The model predictive control (MPC) method is used to solve the problem of optimal control [25]. To relax requirements on the individual UAV's processor capabilities, the centralized mode is adopted in this paper. At each discrete moment, predicting the system's future state evolution through the system model and the predicted future state of the system is used to establish an optimization problem, which is solved online to obtain an optimal control sequence. By repeating the previous process at the next moment, this process will continue repeatedly roll as time goes on. The solution idea is shown in Figure 1.

Figure 2 shows the control structure of multi-UAVs' coordinated tracking target based on information theory. By determining the optimal control $\mathbf{u}_{i,k}^*$ of UAV i at time k, we control UAV i at the optimal observation position. Through the observation of UAV i, the state entropy of the target at the current moment is minimized, thereby obtaining an accurate target state.

Combined with the model predictive control method, the cost function of UAV i for target observation at time k is

$$J_{i,k} = \sum_{m=k}^{k+N_p} L\left(\mathbf{x}_{t,m},\mathbf{x}_{i,m}\right) = \sum_{m=k}^{k+N_p}\left(-\left|\sum_{i=1}^{n} Y_{i,m}\right|\right), \tag{19}$$

where N_P is the predicted number of steps, n is the number of UAVs, $\mathbf{x}_{i,m}$ is the state variable of the UAV i at time m, $\mathbf{x}_{t,m}$ is the target variable of the UAV i at time m, and $L(\mathbf{x}_{t,m},\mathbf{x}_{i,m})$ is the scalar function of the target and the UAV state at time m. Therefore, the multi-UAVs' coordinated target tracking problem is transformed into a problem of optimal control that minimizes the objective function under constraints based on a nonlinear model. The mathematical model is as follows:

$$\begin{aligned} &\min_{\mathbf{u}_{i,k}^*} J_{i,k}, \\ &s.t.\ \mathbf{x}_{i,k+1} - f_d\left(\mathbf{x}_{i,k},\mathbf{u}_{i,k}\right) = 0, \\ &S_v\left(\mathbf{u}_{i,k}\right) = \frac{\left|u_{i,vk} - v_0\right| - v_{\max}}{v_{\max}} \le 0, \\ &S_\omega\left(\mathbf{u}_{i,k}\right) = \frac{\left|u_{i,\omega k}\right| - \omega_{\max}}{\omega_{\max}} \le 0, \end{aligned} \tag{20}$$

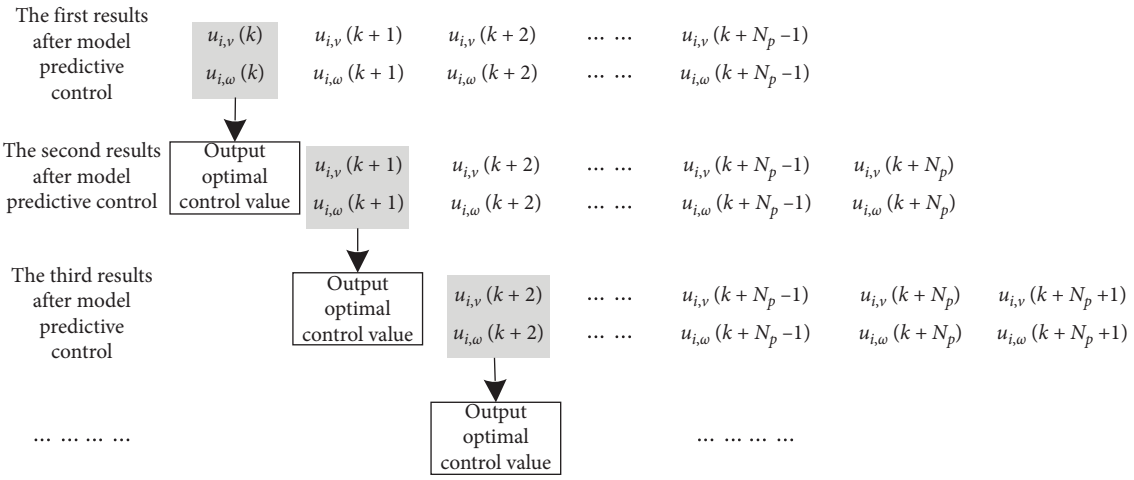

Figure 1: Diagram of model predictive control output.

where $\mathbf{u}_{i,k}$ is the control input variable of the UAV i at time k.

3.3. Optimal Control Solution. To solve the problem of (20), the Lagrange multiplier vector λ is first introduced, and $\lambda = [\lambda_1, \lambda_2, \lambda_3, \lambda_4, \lambda_5]^T$ based on the state of the UAV is five-dimensional. The optimal control problem of multi-UAVs' system coordinated target tracking can be attributed to the problem of minimizing the following performance function by introducing a penalty factor μ_v and μ_w.

$$J_{i,k} = \sum_{m=k}^{k+N_p} L\left(\mathbf{x}_{t,m}, \mathbf{x}_{i,m}\right) + \sum_{m=k}^{k+N_p-1} \left\{\boldsymbol{\lambda}_{m+1}^T \left(f\left(\mathbf{x}_{i,m}, \mathbf{u}_{i,m}\right) - \mathbf{x}_{i,m+1}\right) + \mu_v l_{v,m} S_v\left(\mathbf{u}_{i,m}\right) + \mu_\omega l_{\omega,m} S_\omega\left(\mathbf{u}_{i,m}\right)\right\},\ k = 1, 2, \ldots, N,$$
$$l_{*,m} = \begin{cases} 0, & S_{*,m} \le 0, \\ 1, & S_{*,m} > 0, \end{cases} \tag{21}$$

$l_{*,m}$ shows that the penalty function is zero when the control variable meets the constraint; otherwise, the penalty function is sufficiently large.

Let us define the Hamiltonian function as

$$H_{i,m} = L\left(\mathbf{x}_{t,m}, \mathbf{x}_{i,m}\right) + \boldsymbol{\lambda}_{m+1}^T f\left(\mathbf{x}_{i,m}, \mathbf{u}_{i,m}\right) + \mu_v l_{v,m} S_v\left(\mathbf{u}_{i,m}\right) + \mu_\omega l_{\omega,m} S_\omega\left(\mathbf{u}_{i,m}\right),\ m = k, k+1, \ldots, k+N_p-1. \tag{22}$$

We can get

$$\begin{aligned} J_{i,k} &= L\left(\mathbf{x}_{t,k+N_p}, \mathbf{x}_{i,k+N_p}\right) + \sum_{m=k}^{k+N_p-1} \left\{H_{i,m} - \boldsymbol{\lambda}_{m+1}^T \mathbf{x}_{i,m+1}\right\} \\ &= L\left(\mathbf{x}_{t,k+N_p}, \mathbf{x}_{i,k+N_p}\right) - \boldsymbol{\lambda}_{k+N_p}^T \mathbf{x}_{i,k+N_p} + \boldsymbol{\lambda}_k^T \mathbf{x}_{i,k} \\ &\quad + \sum_{m=k}^{k+N_p-1} \left\{H_{i,m} - \boldsymbol{\lambda}_m^T \mathbf{x}_{i,m}\right\}. \end{aligned} \tag{23}$$

We perform first variation on (23) to get

$$\begin{aligned} \delta J_{i,k} &= \left[\frac{\partial L\left(\mathbf{x}_{t,k+N_p}, \mathbf{x}_{i,k+N_p}\right)}{\partial \mathbf{x}_{i,k+N_p}} - \boldsymbol{\lambda}_{k+N_p}^T\right]^T \delta \mathbf{x}_{i,k+N_p} + \boldsymbol{\lambda}_k^T \delta \mathbf{x}_{i,k} \\ &\quad + \sum_{m=k}^{k+N_p-1} \left\{\left[\frac{\partial H_{i,m}}{\partial \mathbf{x}_{i,m}} - \boldsymbol{\lambda}_m^T\right]^T \delta \mathbf{x}_{i,m} + \left[\frac{\partial H_{i,m}}{\partial \mathbf{u}_{i,m}}\right]^T \delta \mathbf{u}_{i,m}\right\}. \end{aligned} \tag{24}$$

The necessary conditions for achieving optimal control are

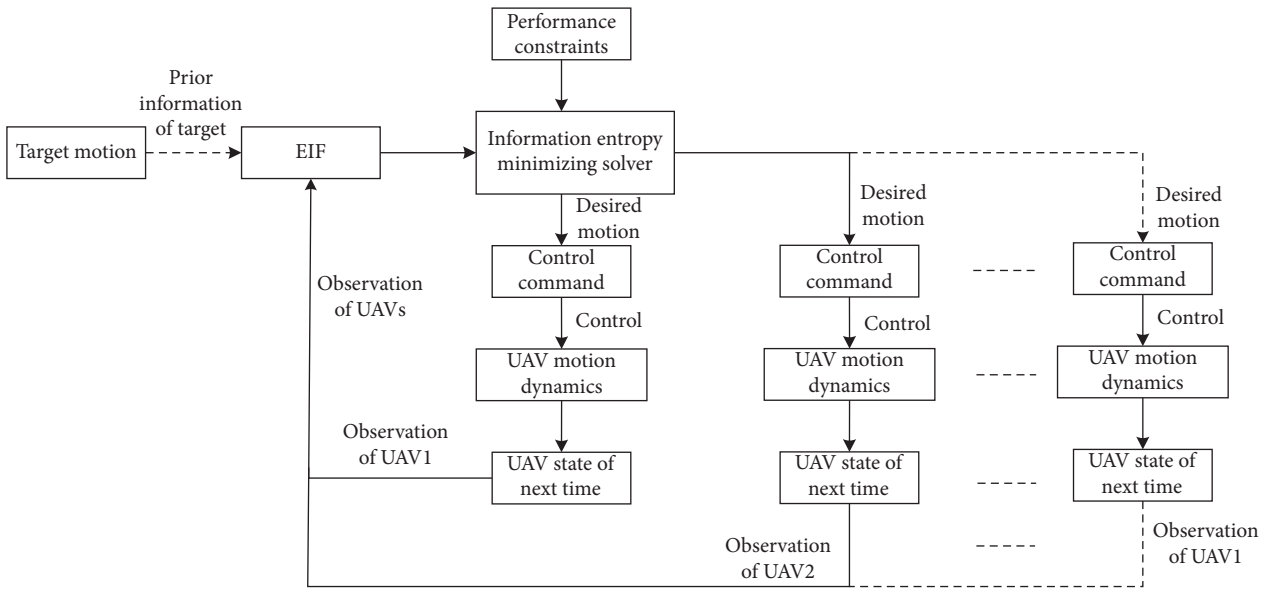

Figure 2: Information-theoretic and NMPC tracking control structure.

$$\boldsymbol{\lambda}_{k+N_p}^{T} = \frac{\partial L\left(\mathbf{x}_{t,k+N_p}, \mathbf{x}_{i,k+N_p}\right)}{\partial \mathbf{x}_{i,k+N_p}}, \tag{25}$$

$$\boldsymbol{\lambda}_{m} = \frac{\partial H_{i,m}}{\partial \mathbf{x}_{i,m}}, \tag{26}$$

where

$$\frac{\partial H_{i,m}}{\partial \mathbf{x}_{i,m}} = \frac{\partial L\left(\mathbf{x}_{t,m}, \mathbf{x}_{i,m}\right)}{\partial \mathbf{x}_{i,m}} + \frac{\partial f^{T}\left(\mathbf{x}_{i,m}, \mathbf{u}_{i,m}\right)}{\partial \mathbf{x}_{i,m}} \boldsymbol{\lambda}_{m+1}. \tag{27}$$

Let $\mathbf{Y} = \sum_{i=1}^{n} \mathbf{Y}_{i,m}$, we can get $L(\mathbf{x}_{t,m}, \mathbf{x}_{i,m}) = -|\mathbf{Y}|$. It can be seen from the relationship between derivative and differential that

$$dL\left(\mathbf{x}_{t,m}, \mathbf{x}_{i,m}\right) = \operatorname{trace}\left(\frac{\partial L\left(\mathbf{x}_{t,m}, \mathbf{x}_{i,m}\right)^{T}}{\partial |\mathbf{Y}|} d|\mathbf{Y}|\right). \tag{28}$$

From the formula $d(|\mathbf{Y}|) = |\mathbf{Y}| \operatorname{trace}(\mathbf{Y}^{-1} d\mathbf{Y})$, we can know that

$$\begin{aligned} dL\left(\mathbf{x}_{t,m}, \mathbf{x}_{i,m}\right) &= \operatorname{trace}\left(\frac{\partial L\left(\mathbf{x}_{t,m}, \mathbf{x}_{i,m}\right)^{T}}{\partial |\mathbf{Y}|} d|\mathbf{Y}|\right) \\ &= -\operatorname{trace}(d|\mathbf{Y}|) \\ &= -\operatorname{trace}\left(|\mathbf{Y}| \operatorname{trace}\left(\mathbf{Y}^{-1} d\mathbf{Y}\right)\right) \\ &= -\operatorname{trace}\left(|\mathbf{Y}| \operatorname{trace}\left(2\mathbf{R}_{i,m}^{-1} \mathbf{H}_{x_{t,m}} \mathbf{Y}^{-1} \frac{\partial \mathbf{H}_{x_{t,m}}}{\partial \mathbf{x}_{i,m}} d\mathbf{x}_{i,m}\right)\right) \\ &= -\operatorname{trace}\left(|\mathbf{Y}| \operatorname{trace}\left(\left(\left(2\mathbf{R}_{i,m}^{-1} \mathbf{H}_{x_{t,m}} \mathbf{Y}^{-1}\right)^{T}\right)^{T} \frac{\partial \mathbf{H}_{x_{t,m}}}{\partial \mathbf{x}_{i,m}} d\mathbf{x}_{i,m}\right)\right). \end{aligned} \tag{29}$$

According to formula $\operatorname{trace}(\mathbf{A}^{T}\mathbf{B}) = (\operatorname{vec}\mathbf{A})^{T} \operatorname{vec}(\mathbf{B})$, (29) becomes

$$dL\left(\mathbf{x}_{t,m}, \mathbf{x}_{i,m}\right) = -|\mathbf{Y}| \operatorname{trace}\left(\left(\operatorname{vec}\left(2\mathbf{R}_{i,m}^{-1} \mathbf{H}_{x_{t,m}} \mathbf{Y}^{-1}\right)^{T}\right)^{T} \operatorname{vec}\left(\frac{\partial \mathbf{H}_{x_{t,m}}}{\partial \mathbf{x}_{i,m}} d\mathbf{x}_{i,m}\right)\right), \tag{30}$$

where trace$(\cdot)$ represents the trace of the matrix and vec$(\cdot)$ represents the column vectorization of the matrix.

According to the relationship between derivative and differential, we can get the following:

$$dL\left(\mathbf{x}_{t,m}, \mathbf{x}_{i,m}\right) = \operatorname{trace}\left(\frac{\partial L\left(\mathbf{x}_{t,m}, \mathbf{x}_{i,m}\right)^T}{\partial \mathbf{x}_{i,m}} d\mathbf{x}_{i,m}\right). \tag{31}$$

Combining (30) and (31), we can see that

$$\begin{aligned}\frac{\partial L\left(\mathbf{x}_{t,m}, \mathbf{x}_{i,m}\right)}{\partial \mathbf{x}_{i,m}} &= -2|\mathbf{Y}|\left\{\left[\operatorname{vec}\left(\mathbf{R}_{i,m}^{-1}\mathbf{H}_{x_{t,m}}\mathbf{Y}^{-1}\right)\right]^T \frac{\partial \operatorname{vec}\mathbf{H}_{x_{t,m}}}{\partial \mathbf{x}_{i,m}^T}\right\}^T \\ &= 2L\left(\mathbf{x}_{t,m}, \mathbf{x}_{i,m}\right)\left\{\left[\operatorname{vec}\left(\mathbf{R}_{i,m}^{-1}\mathbf{H}_{x_{t,m}}\left(\sum_{i=1}^{n}\mathbf{Y}_{i,m}\right)^{-1}\right)\right]^T \frac{\partial \operatorname{vec}\mathbf{H}_{x_{t,m}}}{\partial \mathbf{x}_{i,m}^T}\right\}^T,\end{aligned} \tag{32}$$

where

$$\mathbf{H}_{x_{t,l}} = \frac{\partial h_i\left(\mathbf{x}_k, \mathbf{x}_{t,k}\right)}{\partial \mathbf{x}_{l,k}^T} = \begin{bmatrix} \frac{\Delta x_{i,k}}{r_{i,k}} & 0 & \frac{\Delta y_{i,k}}{r_{i,k}} & 0 \\ -\frac{\Delta y_{i,k}}{r_{i,k}^2} & 0 & \frac{\Delta x_{i,k}}{r_{i,k}^2} & 0 \end{bmatrix},$$

$$\frac{\partial \operatorname{vec}\mathbf{H}_{x_{t,l}}}{\partial \mathbf{x}_{i,l}^T} = \frac{1}{r_{i,k}^4}\begin{bmatrix} -\Delta y_{i,k}^2 r_{i,k} & \Delta x_{i,k}\Delta y_{i,k} r_{i,k} & 0 & 0 & 0 \\ -2\Delta x_{i,k}\Delta y_{i,k} & \Delta x_{i,k}^2 - \Delta y_{i,k}^2 & 0 & 0 & 0 \\ 0 & 0 & 0 & 0 & 0 \\ 0 & 0 & 0 & 0 & 0 \\ \Delta x_{i,k}\Delta y_{i,k} r_{i,k} & -\Delta x_{i,k}^2 r_{i,k} & 0 & 0 & 0 \\ \Delta x_{i,k}^2 - \Delta y_{i,k}^2 & 2\Delta x_{i,k}\Delta y_{i,k} & 0 & 0 & 0 \\ 0 & 0 & 0 & 0 & 0 \\ 0 & 0 & 0 & 0 & 0 \end{bmatrix}, \tag{33}$$

$$\frac{\partial f\left(\mathbf{x}_{i,l}, \mathbf{u}_{i,l}\right)}{\partial \mathbf{x}_{i,l}} = \begin{bmatrix} 1 & 0 & -v_{i,l}\sin\varphi_{i,l}T_s & \cos\varphi_{i,l}T_s & 0 \\ 0 & 1 & v_{i,l}\cos\varphi_{i,l}T_s & \sin\varphi_{i,l}T_s & 0 \\ 0 & 0 & 1 & 0 & T_s \\ 0 & 0 & 0 & 1 - \frac{T_s}{\tau_v} & 0 \\ 0 & 0 & 0 & 0 & 1 - \frac{T_s}{\tau_\omega} \end{bmatrix}.$$

Equation (24) becomes

$$\delta J_{i,k} = \boldsymbol{\lambda}_k^T \delta \mathbf{x}_{i,k} + \sum_{m=k}^{k+N_p-1}\left[\frac{\partial H_{i,m}}{\partial \mathbf{u}_{i,m}}\right]^T \delta \mathbf{u}_{i,m}. \tag{34}$$

Using the gradient descent method to iteratively optimize the cost function, we get

$$\mathbf{u}_{i,m}^{t+1} = \mathbf{u}_{i,m}^t - \Delta_{i,m}\frac{\partial H_{i,m}}{\partial \mathbf{u}_{i,m}}, m = k, k+1, \ldots, k+N_p-1, \tag{35}$$

where t is the number of iteration, $\Delta_{i,m}$ is the iteration step, and $\partial H_{i,m}/\partial \mathbf{u}_{i,m}$ is expressed as

$$\begin{aligned}\frac{\partial H_{i,m}}{\partial \mathbf{u}_{i,m}} &= \boldsymbol{\lambda}_{m+1}^T \frac{\partial f\left(\mathbf{x}_{i,m}, \mathbf{u}_{i,m}\right)}{\partial \mathbf{u}_{i,m}} + \mu_v l_{v,m}\frac{\partial S_v\left(\mathbf{u}_{i,m}\right)}{\partial \mathbf{u}_{i,m}} \\ &\quad + \mu_\omega l_{\omega,m}\frac{\partial S_\omega\left(\mathbf{u}_{i,m}\right)}{\partial \mathbf{u}_{i,m}},\end{aligned} \tag{36}$$

$$\frac{\partial f\left(\mathbf{x}_{i,m}, \mathbf{u}_{i,m}\right)}{\partial \mathbf{u}_{i,m}} = \begin{bmatrix} 0 & 0 & 0 & \frac{T_s}{\tau_v} & 0 \\ 0 & 0 & 0 & 0 & \frac{T_s}{\tau_\omega} \end{bmatrix}^T. \tag{37}$$

The iteration is terminated in the existing optimization method [13] when the cost function change is less than a certain threshold. However, this method has a slower convergence speed when the UAV's initial position is far from the target. Therefore, this paper adopts the step size as an iteration termination condition to improve the convergence speed. The step size decreases when the cost function does not decrease but increases in the iterative process. The iteration is terminated when the step size reaches a smaller threshold, and the cost function changes little, indicating that the optimized result is obtained.

In summary, the flow chart of the nonlinear model predictive control algorithm based on information entropy (IENMPC) is shown in Table 1.

4. Simulation Results

The mission of the UAV used in this paper is to observe the remote sea surface target, and it is known that the estimation accuracy depends not only on the filter performance but also on the relative geometry between the unmanned aerial vehicle (UAV) and the target. Therefore, the scenario of two, three, four, and five UAVs cooperating to observe the target is considered in this paper, and the constraint condition that UAV needs to meet is that the velocity and yaw rate of UAV are within the constraint range.

Table 1: Nonlinear model prediction control algorithm based on information entropy (IENMPC).

Current UAV i	Communication	Coordinated UAV
Calculating optimal control of k time Current state of UAV i	$\xrightarrow{Z_i(k)}$	Current state of coordinated UAV.
Observation information of sensor acquires $z_i(k)$	$\xleftarrow{Z(k)}$	Observation information of sensor acquires $z(k)$.
Initialize control sequence $\mathbf{U}0$, cost function $J_{\min}$, predicted number of steps N_P, iteration step $\Delta_{i,k}$, α, ε and t		
While $\Delta_{i,m} > \varepsilon$		While $\Delta_{i,m} > \varepsilon$
UAV state propagation [equation (3)]		.
Information matrix, target estimation state, jacobian matrix, and observation noise matrix were acquired through EIF. [equations (7)–(14)]		.
λ_m computation [equation (25) and (26)]		.
J_i computation [equation (23)].		
$\partial H_{i,m}/\partial \mathbf{u}_{i,m}$ computation [equation (36)]		.
If $J_i < J_{\min}$, $J_{\min} = J_i$		.
else $\Delta_{i,m} = \alpha\Delta_{i,m}$		.
end		.
$\mathbf{u}_{i,m}^{t+1} = \mathbf{u}_{i,m}^{t} - \Delta_{i,m}\partial H_{i,m}/\partial \mathbf{u}_{i,m}$		..
$t = t + 1$		$t = t + 1$
end		End
Calculating the status of UAV at $k+1$ time [equation (3)]		
Calculating optimal control input of $k+1$ time		

Table 2: Initial state information and performance constraints of UAVs.

Number	Initial state	v_0 (m/s)	$\Delta v_{\max}$ (m/s)	$\omega_{\max}$ (rad/s)	Observation error (distance (m), angle (°))
1	(0, 0, 0, 100, 0)	100	10	0.35	[20, 0.3]
2	(1000, 0, 0, 100, 0)	100	10	0.35	[20, 0.3]
3	(2000, 0, 0, 100, 0)	100	10	0.35	[20, 0.3]
4	(−1000, 0, 0, 100, 0)	100	10	0.35	[20, 0.3]
5	(−2000, 0, 0, 100, 0)	100	10	0.35	[20, 0.3]

4.1. Assumptions and Conditions. Experiments were performed using MATLAB R2020a on the computer with CPU processor of Intel Corei7 and dominant frequency of 1.6 GHz. It is assumed that the target is moving with a constant speed at 8.5 m/s, and the mean square deviation of the velocity noise is 0.01 in the horizontal and vertical directions. The initial position of the target is at (80000, 80000). The initial position, speed, and performance parameters of the UAV are shown in Table 2, and the other parameter settings required are shown in Table 3. The simulation time lasts for 1500 s.

4.2. Analysis of Simulation Results. To analyze the feasibility and benefits of the proposed method (IENMPC) in this paper, the same scenarios are discussed with the method of Lyapunov vector field guidance (LVFG), which is expressed as

$$\mathrm{g}(x, y) = \begin{bmatrix} g_x \\ g_y \end{bmatrix} = \begin{bmatrix} \dot{x}_d \\ \dot{y}_d \end{bmatrix} = \left(\frac{v_d}{r\left(r^2 + R_0^2\right)}\right)\begin{bmatrix} -x_r\left(r^2 - R_0^2\right) - y_r\left(2 \cdot r \cdot R_0\right) \\ -y_r\left(r^2 - R_0^2\right) + x_r\left(2 \cdot r \cdot R_0\right) \end{bmatrix}. \tag{38}$$

Obtaining the expected heading angle of the UAV through the vector field guidance, we get

$$\varphi_d = \arctan\left(\frac{\dot{y}_d}{\dot{x}_d}\right). \tag{39}$$

A proportional controller is designed using the principle of feedback control as follows:

$$\begin{aligned} u_\omega &= \dot{\varphi}_d - k_i\left(\varphi_d - \varphi\right), \\ \dot{\varphi}_d &= 4v_d\frac{R_0 r^2}{\left(r^2 + R_0^2\right)^2}, \end{aligned} \tag{40}$$

where $r = \sqrt{(x_i - x_T)^2 + (y_i - y_T)^2} = \sqrt{x_r^2 + y_r^2}$, (x_T, y_T) is the position of the target that can be estimated from the filter, and R_0 is a desired standoff distance from the UAV to

Table 3: Simulation parameters.

Parameter	Value	Unit
T_s	0.5	s
N_p	9	N/A
τ_v, τ_ω	0.5	s
μ_c, μ_w	$1e5$	N/A
ε	0.001	N/A
$J_{\min}$	inf	N/A
Δ	0.05	N/A
α	0.9	N/A

Initial covariance matrix is $P0 = \mathrm{diag}[100, 50, 100, 50]$ in filter and the initial control sequence is $U0 = [100, 0; 100, 0; 100, 0; 100, 0; 100, 0; 100, 0; 100, 0; 100, 0; 100, 0]^T$.

the target. v_d is a desired UAV speed. In this simulation set, $R_0 = 20$ km and $v_d = 110$ m/s.

Figure 3 shows the simulation results of UAV1 and UAV2 when the simulation time lasted for 1500 s. It can be seen from Figures 3(a) and 3(b) that the UAV first performs angular separation so that the angle between the two UAVs and the target approaches 90 degrees and then moves towards the target. Figures 3(c) and 3(d) show the change curve of speed and yaw rate during the UAV flight, respectively. It is easy to see that the yaw rate control command and the speed control command are feasible according to the range of yaw rate, which is within the maximum range ±0.35, and the range of speed is within the maximum variation range ±10 m/s. Another phenomenon is that the UAV flies to the target at the maximum speed of 110 m/s in Figure 3(c) which indicates that the UAV separates the angle and flies to the target in the shortest time to reduce the uncertainty of the target position estimation.

Figure 4(a) shows the trajectories of UAVs planned by the LGVF method and the UAVs directly moving towards the target without angle separation. Figure 4(b) displays the target position's root mean squared error (RMSE) based on the IENMPC method and the LVFG method after 200 Monte Carlo simulations. The average RMSE of the target position is 6.5 m through the IENMPC method. However, the average RMSE of the target is 16.6 m using the LGVF method, and the error converges to 7.2 m until the simulation is in the 1400 s, when the UAV is already close to the target. Figure 4(c) shows the information entropy variation curve of the two methods. It can be seen from Figure 4(c) that the information entropy is −8.76 in the IEMPC method, and the information entropy is −8.02 in the LGVF method when the simulation is 300 s. The information entropy of the IENMPC method converges at −9.29, while the information entropy of the LGVF method maintains around −8.97 in the end. The information entropy of the IEMPC method, which is more accurate in estimating the target state, is significantly smaller than that of the LGVF method. We can conclude that the IENMPC method is better than the LGVF method in the position estimation of the remote marine target.

Figure 5 shows the simulation results of three UAVs when the simulation time lasted for 1500 s. Figure 5(a) displays the trajectory of coordinated tracking of three UAVs. Figure 4(b) shows the line-of-sight angle between three UAVs and the target. UAV2 and UAV3 fly in the same direction for a while at first and then UAV2 turns back and finally moves towards the target to make UAV2 form a 60° angle between UAV1 and the target in Figure 5(b). It can be further obtained that the optimal observation configuration for three UAVs is that the line-of-sight angle between UAV2, UAV 1, and the target is 60 degrees, and the line-of-sight angle between UAV1, UAV3, and the target is 120 degrees from Figure 5(b). From Figures 5(c) and 5(d), UAVs' speed and yaw rate are within the constraint range, proving the proposed method's effectiveness.

The simulation results of four UAVs and five UAVs are shown in Figure 6. The optimal geometric configuration of four UAVs is that the two UAVs fly to the target at 90 degrees. The optimal geometric configuration of the observation of five UAVs is the configuration of 2-2-1. Therefore, the optimal observation geometric configuration is that the UAV formation angle is 90 degrees based on the fact that the number of UAVs is even. The UAV formation angles are 60 degrees and 120 degrees when the number of UAVs is odd for the multi-UAVs' coordinated target tracking problem, which has guiding significance for designing multi-UAVs' flight control laws that maintain the optimal observation configuration.

In Figure 7, the RMSE and information entropy of multi-UAVs' target position estimation are displayed. In Figure 7(a), the RMSE of the target position is decreasing as the number of UAV increases, which indicates that increasing the UAV number can improve the accuracy of target position estimation. However, through Figure 5(b), the information entropy is reduced by 2.83% from two UAVs to three UAVs. It is reduced by 2.41% from three UAVs to four UAVs. The information entropy is only reduced by 1.63% from four UAVs to five UAVs. This result shows that the target position's improvement is getting smaller and smaller as the number of UAVs increases. Considering the use effectiveness and tracking accuracy, observing three UAVs or four UAVs is an excellent choice to track the target.

To analyze the computational efficiency (CPU cost) of the proposed algorithm, the average elapsed time (AET) of the algorithm, the AET of the optimized solution, and the maximum running time of the algorithm are evaluated. The AET of the algorithm refers to the time taken by the algorithm to run once, and the results are shown in Table 4.

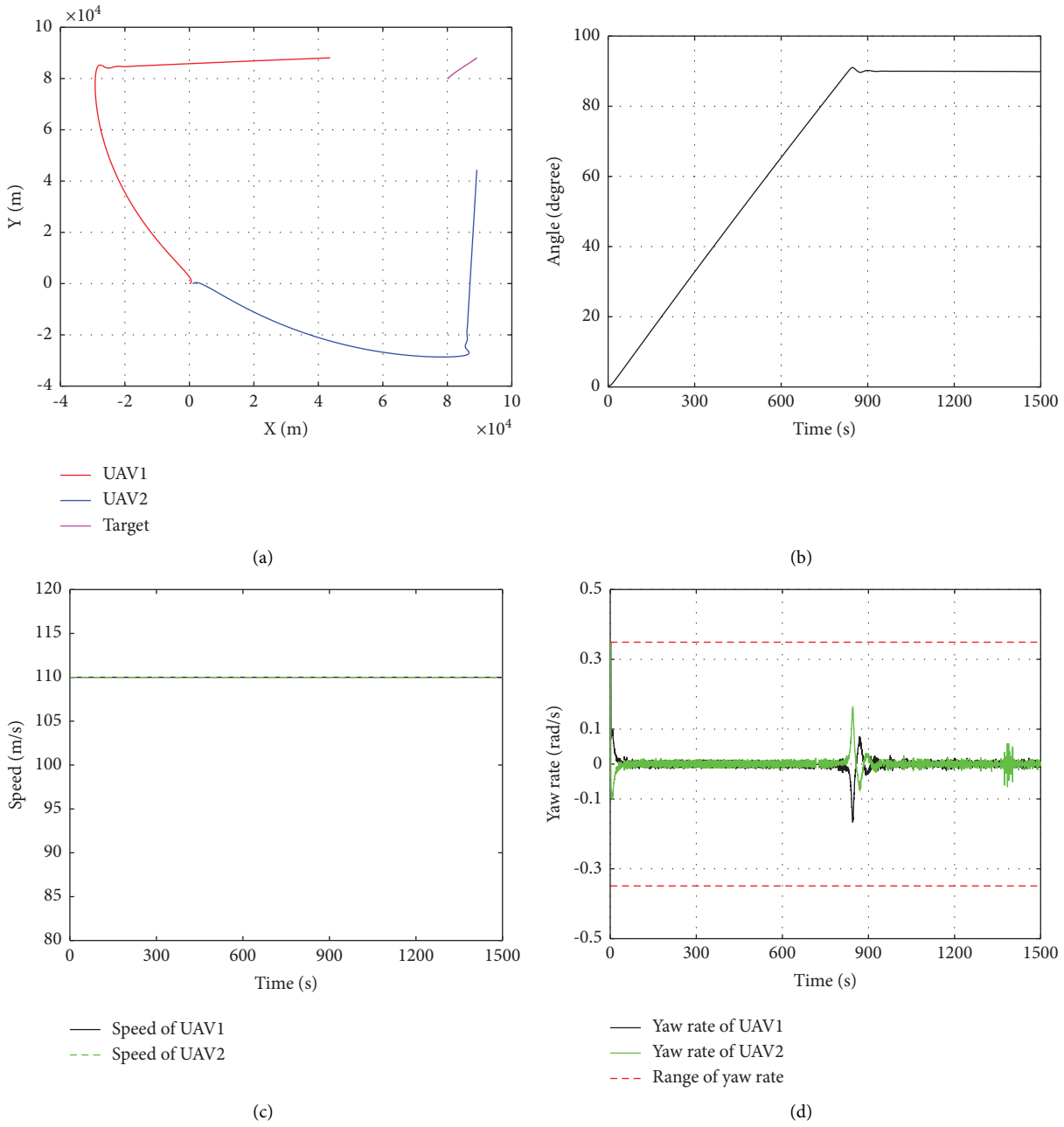

Figure 3: Simulation results of two UAVs. (a) Trajectory of IEMPC method. (b) The line-of-sight angle. (c) The variation curve of speed. (d) The variation curve of yaw rate.

Table 4 shows that the AET of the algorithm, the AET of the optimized solution, and the maximum run time increase with the number of UAVs. However, the maximum run time of UAVs does not exceed 300 ms, which indicates the good real-time performance of the proposed IENMPC method.

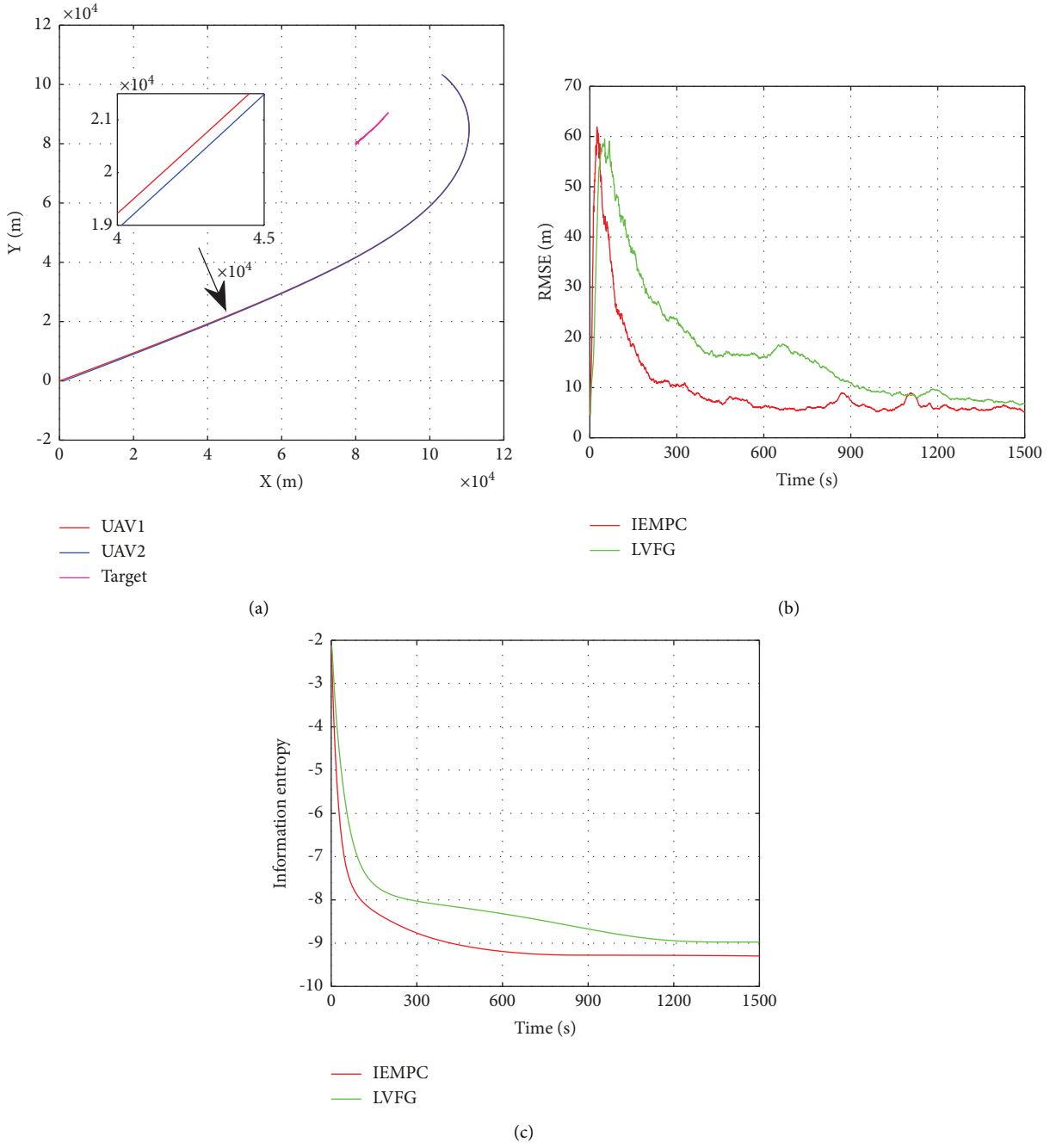

Figure 4: Comparison results of IEMPC and LVFG. (a) Trajectory of LVFG method. (b) RMSE of the target position. (c) Information entropy.

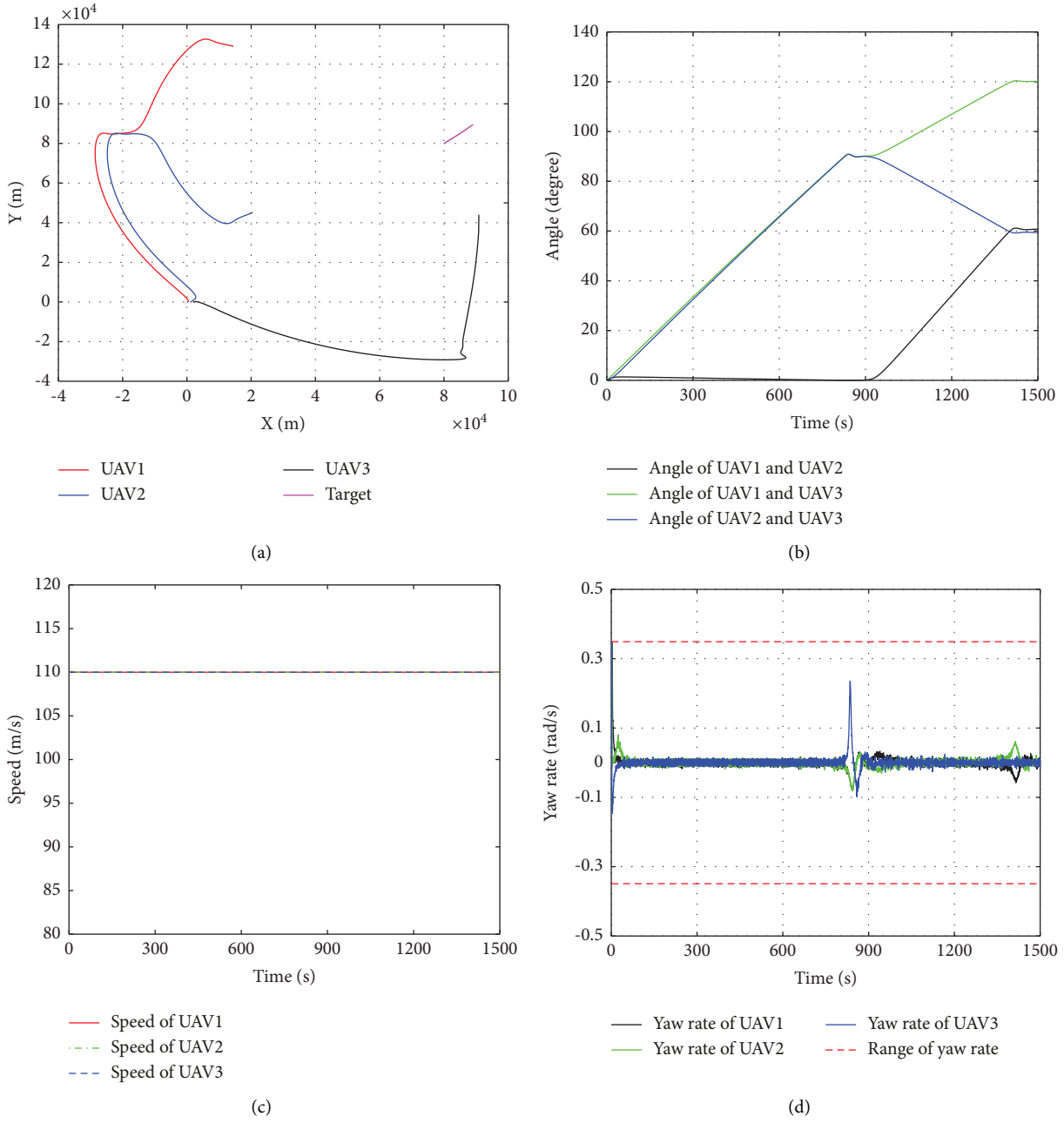

Figure 5: Simulation results of three UAVs. (a) Trajectory of three UAVs. (b) The line-of-sight angle between three UAVs and target. (c) The variation curve of speed. (d) The variation curve of yaw rate.

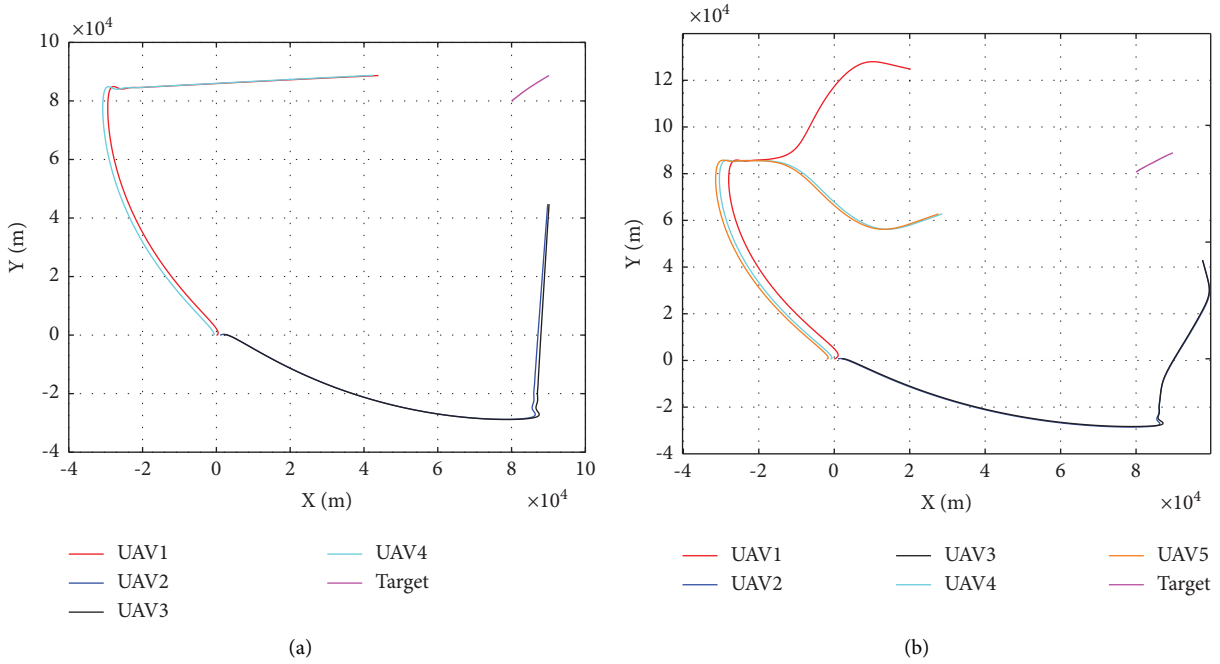

Figure 6: Simulation results of multi-UAVs. (a) Trajectory of four UAVs. (b) Trajectory of five UAVs.

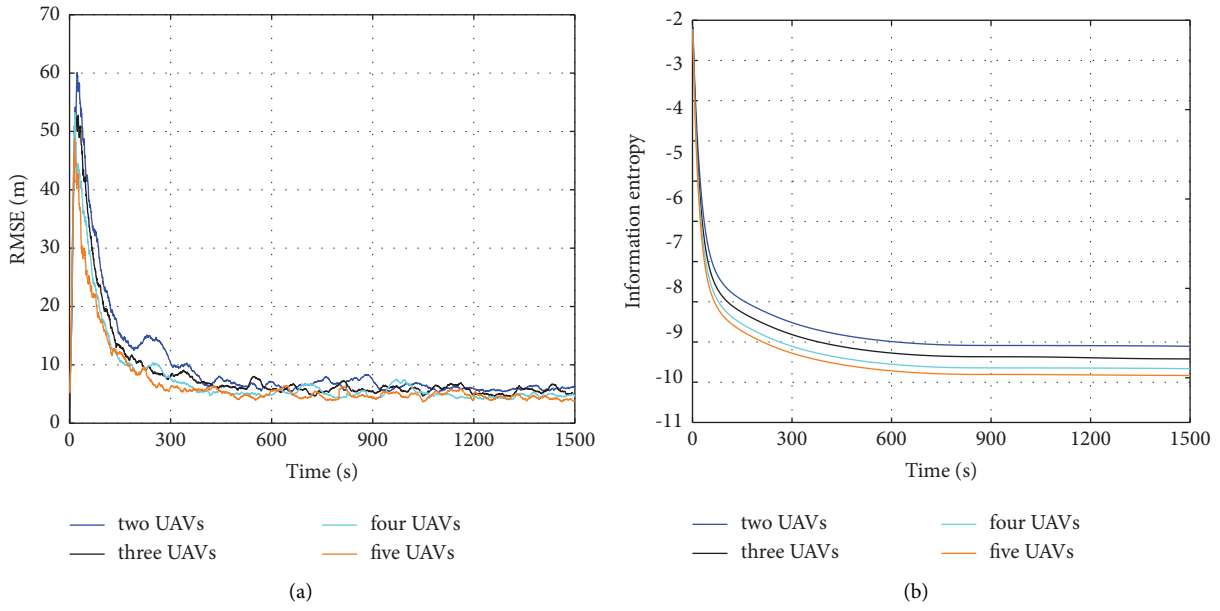

Figure 7: RMSE and information entropy of multi-UAVs. (a) RMSE of the target position. (b) Information entropy.

Table 4: Consume time of the algorithm with different UAVs.

Number of UAVs	The AET of the optimized solution (ms)	The AET of the algorithm (ms)	The maximum running time (ms)
Two UAVs	32.586	62.271	87.673
Three UAVs	38.211	111.793	125.527
Four UAVs	43.476	175.781	210.093
Five UAVs	48.489	241.526	265.688

5. Conclusion

This paper proposed multi-UAVs' coordinated target tracking control method, which uses a nonlinear model predictive control method to minimize the target state's information entropy to obtain an accurate target position. This method's advantage is that it can keep the UAV at the optimal observation position and is easy to extend to the coordinated tracking of multiple UAVs. It can effectively improve the remote marine target tracking performance under the performance constraints of the UAV at the same time. Also, the step size was used as the iterative termination condition to solve the problem of slower convergence speed when the UAV's initial position is far from the target compared with the existing optimization methods. The convergence speed of the optimization method was improved. Comparative simulations of two UAVs with the LVFG method showed the superiority of this method for target positioning. It was possible to obtain the geometric configuration that maintained the optimal observation through the simulation of three UAVs, four UAVs, and five UAVs, which can reference the design of multi-UAVs' flight control law based on the optimal observation configuration.

Future works are planned to extend this method to three-dimensional space because the UAV position is more complex and changeable in three-dimensional space, leading to UAV's optimal observation configuration that significantly impacts target tracking. An additional crucial future work will be performed to consider the factor of time, that is, how to obtain the accurate target state within finite time, which is also the focus of future research.

Data Availability

The data used to support the findings of this study are available from the corresponding authors upon request.

Conflicts of Interest

The authors declare that they have no conflicts of interest.

References

[1] D. Nikolic, N. Stojkovic, Z. Popovic et al., "Maritime over the horizon sensor integration: HFSWR data fusion algorithm," *Remote Sensing*, vol. 11, no. 7, p. 852, 2019.

[2] I. Mahmud and Y. Z. Cho, "Detection avoidance and priority-aware target tracking for UAV group reconnaissance operations," *Journal of Intelligent and Robotic Systems*, vol. 92, no. 2, pp. 381–392, 2018.

[3] Y. Lyu, T. Kang, Q. Pan, C. Zhao, and J. Hu, "UAV sense and avoidance: concepts, technologies, and systems," *SCIENTIA SINICA Informationis*, vol. 49, no. 5, pp. 520–537, 2019.

[4] D. Pack, G. York, and R. Fierro, "Information-based cooperative control for multiple unmanned aerial vehicles," in *Proceedings of the 2006 IEEE International Conference on Networking, Sensing and Control*, pp. 446–450, IEEE, Lauderdale, FL, USA, April 2006.

[5] L. Wang, H. Peng, H. Y. Zhu, and L. C. Shen, "Cooperative tracking of ground moving target using unmanned aerial vehicles in cluttered environment," *Control Theory & Applications*, vol. 28, pp. 300–308, 2011.

[6] S. Zhang, Y. Guo, Z. Lu, S. Wang, and Z. Liu, "Cooperative detection based on the adaptive interacting multiple model-information filtering algorithm," *Aerospace Science and Technology*, vol. 93, Article ID 105310, 2019.

[7] A. N. Bishop, B. Fidan, B. D. Anderson, K. Doğançay, and P. N. Pathirana, "Optimality analysis of sensor-target localization geometries," *Automatica*, vol. 46, no. 3, pp. 479–492, 2010.

[8] Y. Zhong, X. Wu, S. Huang, C. Li, and J. Wu, "Optimality analysis of sensor-target geometries for bearing-only passive localization in three dimensional space," *Chinese Journal of Electronics*, vol. 25, no. 2, pp. 391–396, 2016.

[9] S. Xu and K. Dogançay, "Optimal sensor placement for 3-D angle-of-arrival target localization," *IEEE Transactions on Aerospace and Electronic Systems*, vol. 53, no. 3, pp. 1196–1211, 2017.

[10] B. Grocholsky, A. Makarenko, and H. Durrant-Whyte, "Information-theoretic coordinated control of multiple sensor platforms," in *Proceedings of the 2003 IEEE International Conference on Robotics and Automation (Cat. No. 03CH37422)*, vol. 1, pp. 1521–1526, IEEE, Taipei, Taiwan, September 2003.

[11] G. M. Hoffmann and C. J. Tomlin, "Mobile sensor network control using mutual information methods and particle filters," *IEEE Transactions on Automatic Control*, vol. 55, no. 1, pp. 32–47, 2010.

[12] D. Darmon, "Information-theoretic model selection for optimal prediction of stochastic dynamical systems from data," *Physical Review*, vol. 97, no. 3, Article ID 032206, 2018.

[13] S. Uluskan, "Noncausal trajectory optimization for real-time range-only target localization by multiple UAVs," *Aerospace Science and Technology*, vol. 99, Article ID 105558, 2020.

[14] G. Tang, Z. Hou, C. Claramunt, and X. Hu, "UAV trajectory planning in a port environment," *Journal of Marine Science and Engineering*, vol. 8, p. 592, 2020.

[15] E. W. Frew, D. A. Lawrence, and S. Morris, "Coordinated standoff tracking of moving targets using Lyapunov guidance vector fields," *Journal of Guidance, Control, and Dynamics*, vol. 31, no. 2, pp. 290–306, 2008.

[16] S. Lim, Y. Kim, D. Lee, and H. Bang, "Standoff target tracking using a vector field for multiple unmanned aircrafts," *Journal of Intelligent and Robotic Systems*, vol. 69, no. 1-4, pp. 347–360, 2013.

[17] W. Jung, S. Lim, D. Lee, and H. Bang, "Unmanned aircraft vector field path following with arrival angle control," *Journal of Intelligent and Robotic Systems*, vol. 84, no. 1-4, pp. 311–325, 2016.

[18] A. J. Sinclair, R. J. Prazenica, and D. E. Jeffcoat, "Optimal and feedback path planning for cooperative attack," *Journal of Guidance, Control, and Dynamics*, vol. 31, no. 6, pp. 1708–1715, 2008.

[19] S. Zhao, Z. Li, and Z. Ding, "Bearing-only formation tracking control of multiagent systems," *IEEE Transactions on Automatic Control*, vol. 64, no. 11, pp. 4541–4554, 2019.

[20] C. Hu, Z. Zhang, Y. Tao, and N. Wang, "Decentralized real-time estimation and tracking for unknown ground moving target using UAVs," *IEEE Access*, vol. 7, pp. 1808–1817, 2019.

[21] W. Wang, P. Bai, Y. Wang, X. Liang, and J. Zhang, "Optimal sensor deployment and velocity configuration with hybrid

TDOA and FDOA measurements," *IEEE Access*, vol. 7, Article ID 109181, 2019.

[22] H. Oh and S. Kim, "Persistent standoff tracking guidance using constrained particle filter for multiple UAVs," *Aerospace Science and Technology*, vol. 84, pp. 257–264, 2019.

[23] S. Jiao, J. Du, Y. Li, and Y. Li, "Target Filter tracking algorithm based on IABBSCA-IMM," *Mathematical Problems in Engineering*, vol. 2022, Article ID 8160970, 11 pages, 2022.

[24] P. Chen, H. Ma, S. Gao, and Y. Huang, "Modified extended Kalman filtering for tracking with insufficient and intermittent observations," *Mathematical Problems in Engineering*, vol. 2015, Article ID 981727, 9 pages, 2015.

[25] H. Degachi, B. Naffeti, W. Chagra, and M. Ksouri, "Filled function method for nonlinear model predictive control," *Mathematical Problems in Engineering*, vol. 2018, Article ID 9497618, 8 pages, 2018.